



VEGF-A inhibits agonist-mediated Ca^{2+} responses and activation of IK_{Ca} channels in mouse resistance artery endothelial cells

Xi Ye¹ , Taylor Beckett^{1,2}, Pooneh Bagher^{1,3}, Christopher J. Garland¹ and Kim A. Dora¹ 

¹Department of Pharmacology, University of Oxford, Mansfield Road, Oxford, UK

²School of Biomedical Sciences, University of Queensland, Brisbane, Australia

³Department of Medical Physiology, College of Medicine, Texas A&M University Health Science Center, Bryan, TX, USA

Edited by: Kim Barrett and Livia Hool

Key points

- Prolonged exposure to vascular endothelial growth factor A (VEGF-A) inhibits agonist-mediated endothelial cell Ca^{2+} release and subsequent activation of intermediate conductance Ca^{2+} -activated K^+ (IK_{Ca}) channels, which underpins vasodilatation as a result of endothelium-dependent hyperpolarization (EDH) in mouse resistance arteries.
- Signalling via mitogen-activated protein/extracellular signal-regulated kinase kinase (MEK) downstream of VEGF-A was required to attenuate endothelial cell Ca^{2+} responses and the EDH-vasodilatation mediated by IK_{Ca} activation.
- VEGF-A exposure did not modify vasodilatation as a result of the direct activation of IK_{Ca} channels, nor the pattern of expression of inositol 1,4,5-trisphosphate receptor 1 within endothelial cells of resistance arteries.
- These results indicate a novel role for VEGF-A in resistance arteries and suggest a new avenue for investigation into the role of VEGF-A in cardiovascular diseases.

Abstract Vascular endothelial growth factor A (VEGF-A) is a potent permeability and angiogenic factor that is also associated with the remodelling of the microvasculature. Elevated VEGF-A levels are linked to a significant increase in the risk of cardiovascular dysfunction, although it is unclear how VEGF-A has a detrimental, disease-related effect. Small resistance arteries are central determinants of peripheral resistance and endothelium-dependent hyperpolarization (EDH) is the predominant mechanism by which these arteries vasodilate. Using isolated, pressurized resistance arteries, we demonstrate that VEGF-A acts via VEGF receptor-2 (R2) to inhibit both endothelial cell (EC) Ca^{2+} release and the associated EDH vasodilatation mediated by intermediate conductance Ca^{2+} -activated K^+ (IK_{Ca}) channels. Importantly, VEGF-A had no direct effect against IK_{Ca} channels. Instead, the inhibition was crucially reliant on the downstream activation

Xi Ye received his PhD in Ophthalmology from the University of Bristol, UK, in 2015. Subsequently, he took up a postdoctoral position with Professor Kim Dora and Professor Chris Garland at the University of Oxford, UK, where he developed his interests in vasomotor regulation and its contributions towards health and disease. He is hoping to use both molecular and physiological approaches to investigate the pathogenesis and treatments for cardiovascular disease.



of the mitogen-activated protein/extracellular signal-regulated kinase kinase 1/2 (MEK1/2). The distribution of EC inositol 1,4,5-trisphosphate (IP₃) receptor-1 (R1) was not affected by exposure to VEGF-A and we propose an inhibition of IP₃R1 through the MEK pathway, probably via ERK1/2. Inhibition of EC Ca²⁺ via VEGFR2 has profound implications for EDH-mediated dilatation of resistance arteries and could provide a mechanism by which elevated VEGF-A contributes towards cardiovascular dysfunction.

(Resubmitted 19 April 2018; accepted after revision 15 May 2018; first published online 3 June 2018)

Corresponding author K. A. Dora and C. J. Garland: Department of Pharmacology, University of Oxford, Mansfield Road, Oxford OX1 3QT, UK. Emails: kim.dora@pharm.ox.ac.uk and christopher.garland@pharm.ox.ac.uk

Introduction

Vascular endothelial growth factor A (VEGF-A) is a pro-survival, angiogenic and permeability factor acting on endothelial cells (ECs) (Simons, Gordon and Claesson-welsh, 2016). Although there are two receptors for VEGF-A, its effects are mediated primarily through VEGF receptor-2 (R2), whereas VEGF receptor-1 (R1) merely acts as a decoy receptor in ECs, at least in the context of angiogenesis (Fong *et al.* 1995). On binding to VEGF-A, VEGFR2 dimerizes and activates a number of pathways such as mitogen-activated protein (MAP)/extracellular signal-regulated kinase (ERK) kinase 1/2 (MEK1/2)-ERK1/2, phosphatidylinositol-4,5-bisphosphate 3-kinase-Akt and MKK3/4/6-p38 MAP kinase to initiate a range of cellular effects, including DNA synthesis, cell proliferation and an increase in permeability (Simons, Gordon and Claesson-welsh, 2016). However, VEGFR2 dimerization appears only to explain part of the activation signal. In some cases, amplification of the signal occurs through the recruitment and binding of VEGF-A to a co-receptor, neuropilin-1, enabling full activation of downstream pathways (Soker *et al.* 1998; Kawamura *et al.* 2008).

Although VEGF-A is considered to stimulate the generation of nitric oxide (NO) from ECs leading to arterial vasodilatation (Ku *et al.* 1993; Itoh *et al.* 2002), the link between this signal and VEGFR is not clear. In human umbilical vein ECs (HUVECs), VEGF-A increases EC intracellular Ca²⁺ ([Ca²⁺]_i) through the activation of phospholipase C_γ and the subsequent production of inositol 1,4,5-trisphosphate (IP₃) (Favia *et al.* 2014). By contrast, in human microvasculature ECs (HMVECs), the increase in [Ca²⁺]_i appears not to rely on IP₃Rs but, instead, on Ca²⁺ influx through a receptor-operated transient receptor potential channel (Cheng *et al.* 2006; Hamdollah Zadeh *et al.* 2008). An increase in EC Ca²⁺ will potentially activate NO synthase. However, to date, there has been no study linking a VEGF-A evoked rise in EC Ca²⁺ and the release of NO in intact pressurized arteries.

In general, elevation of EC [Ca²⁺]_i activates at least two distinct EC-dependent vasodilator responses: one via NO

release and the other as a result of endothelium-derived hyperpolarization (EDH) with the EDH response predominating in smaller resistance arteries (Garland and Dora, 2017). In the latter, an increase in EC [Ca²⁺]_i stimulates the opening of the small and intermediate conductance Ca²⁺-activated K⁺ channels (SK_{Ca}, IK_{Ca}), which are localized to the endothelium. This results in an efflux of K⁺, causing hyperpolarization of the ECs. The hyperpolarizing current then spreads from the ECs to the neighbouring vascular smooth muscle cells (VSMC) via myoendothelial gap junctions to reduce the open probability of voltage-dependent Ca²⁺ channels, causing vasodilatation (Edwards *et al.* 1998; Dora *et al.* 2008). EC-dependent vasodilatation helps the maintenance of blood flow and ensures sufficient oxygen and nutrients are delivered to tissues. Reduced endothelium-dependent vasodilatation occurs in a number of conditions, including diabetes, cancer and peripheral arterial disease (Lim *et al.* 2004; Stehr *et al.* 2010; Goel and Mercurio, 2013).

In the present study, we provide evidence to suggest that prolonged exposure to VEGF-A and activation of the MEK1/2 pathway lead to a reduction in EC-dependent vasodilatation in mouse isolated resistance arteries and that this reduction reflects a change in EC Ca²⁺ handling and reduced K_{Ca} activity.

Methods

Ethical approval

Ethical approval was obtained and all animal procedures were carried out in accordance with the UK Home Office Animals (Scientific Procedures) Act 1986. Experiments were carried out according to the guidelines laid down by the institution's animal welfare committee and regulations described in the *Journal of Physiology* editorial (Grundy, 2015).

Animals and tissue preparation

Wild-type male C57BL/6J mice (Charles River, Kent, UK) between the ages of 11 and 16 weeks were used in the

present study. Animals were housed in individually ventilated cages under a 12:12 h light/dark cycle and at 20–22°C. Standard chow and water were available *ad libitum*. Mice were killed in accordance with schedule 1 of the Animals (Scientific Procedures) Act by increasing the concentration of CO₂ followed by cervical dislocation as confirmation of death. The mesentery was collected in cold MOPS buffer containing (in mM): 142.5 NaCl, 4.7 KCl, 1 CaCl₂, 1.17 MgSO₄, 3.0 MOPS, 1.2 NaH₂PO₄ (H₂O), 11.0 glucose, 2.0 pyruvate and 0.02 EDTA at pH 7.40 ± 0.02.

Artery isolation and pressure myography

Third-order mesenteric resistance arteries were dissected free of adhering adipocytes and connective tissue. Arteries were cannulated onto glass micropipettes (external diameter 100–120 μm), secured with 11-0 sutures in a 2.0 mL temperature-regulated chamber. Arteries were warmed to 37°C, gradually pressurized to a physiological pressure of 60 mmHg and allowed to equilibrate for 30 min (Beleznaï *et al.* 2011). Agents were applied to the bath, except when VEGF-A was perfused into the lumen. ZM323881 or UO126 were added to the bath 20 min prior to perfusion of either VEGF-A and ZM323881 (VEGFR2 tyrosine kinase inhibitor) or VEGF-A and UO126 (MEK1/2 inhibitor), respectively, into the lumen of artery at 1 μL min⁻¹ using a beehive syringe pump. In preliminary experiments, 250 nM carboxyfluorescein was pumped together with VEGF-A to establish the delay in delivering VEGF-A into the lumen of arteries (15 min at 1 μL min⁻¹). This time was added to the overall pumping time, meaning that $t = 0$ min was the time at which VEGF-A reached the lumen. The luminal flow was stopped immediately prior to obtaining concentration–response curves.

Because the level of VEGF-A ranges from undetectable to 0.1 nM under physiological conditions (Larsson, Sködenberg and Eericson, 2002), rising to several nanomolar in pathological situations (Baker *et al.* 1995; Kaess *et al.* 2016), we compared responses to 1 pM, 0.1 nM and 1 nM VEGF-A. Although VEGFR2 is phosphorylated within 5 min after VEGF-A application, activation of downstream pathways varies from 10 to 60 min (Jang *et al.* 2017). Therefore, arteries were perfused for 60 min.

Diameter measurements were recorded on the stage of an inverted microscope (IX 70; Olympus, Tokyo, Japan) attached to a confocal scanning unit (FV500; Olympus). Artery viability was assessed with contraction to 1–3 μM phenylephrine (PE) followed by endothelium-dependent vasodilatation to 1–10 μM SLIGRL, a PAR2 activating peptide (McGuire *et al.* 2002; Dora *et al.* 2003; Beleznaï *et al.* 2011). Only arteries with dilatation >90% to 3 μM SLIGRL, reflecting undamaged endothelium, were used for the subsequent experiments. The outer diameter

of the artery was measured using MetaMorph, version 7.7.4.0 (Molecular Devices, Sunnyvale, CA, USA). % Dilatation = $(D - D_{\text{constricted}})/(D_{\text{max}} - D_{\text{constricted}}) \times 100$.

EC [Ca²⁺]_i measurement in pressurized arteries

EC Ca²⁺ investigations were conducted on third-order mesenteric resistance arteries from transgenic mice on a C57Bl/6J background expressing the genetically encoded Ca²⁺ indicator, GCaMP2, under the control of a connexin40 promoter [Tg(RP24-25504-GCaMP2)1 Mik mice] (Bagher, Davis and Segal, 2011). The mesenteric artery was isolated and pressurized as described above. Ca²⁺ measurements were taken from ECs at the bottom of the pressurized artery and images were obtained using a 40× water immersion objective (40×/1.15 NA objective, working distance = 0.25 mm; Olympus; excitation 488 nm, emission >505 nm) and acquired using Olympus FluoView 1200 software (FV10-ASW) at ~3 Hz with a gallium arsenide phosphide detector.

Ca²⁺ data were analysed using subcellular regions of interest as described previously (Garland *et al.* 2017), with each event categorized when viewing the original movie file during manual frame-by-frame playback. If a response radiated from a single point and was also synchronized and rapidly decayed within 20 μm², this was termed local; Ca²⁺ waves were defined as asynchronous events that visibly propagated at least 20 μm along the length of an EC. All cells within a field of view (7–11 cells) were manually and individually analysed for Ca²⁺ event frequency. Results are presented as either frequency (events min⁻¹) or F/F_0 traces, with the latter calculated by dividing the fluorescence intensity (F) by an average baseline fluorescence intensity (F_0). The number of local or propagating events were expressed as a percentage of total events.

Immunohistochemistry

Pressurized arteries were fixed with 2% paraformaldehyde for 10 min, blocked and permeabilized with 1% BSA in PBS-Tween 20 (0.1%) for 1 h in luminal and abluminal space. Arteries were labelled with 2 μg mL⁻¹ rabbit anti-IP₃R1 (PA1-901; ThermoFisher Scientific, Waltham, MA, USA) and 2 μg mL⁻¹ mouse anti-ZO-1 (339-100; ThermoFisher Scientific) antibodies in 1% BSA PBS-Tween 20 overnight at 4°C. This was followed by 2 h of incubation with 2 μg mL⁻¹ goat anti-rabbit 488 and anti-mouse 405 secondary antibodies in 1% BSA PBS-Tween 20. The nuclei and elastic lamina were labelled with 15 μM propidium iodide and 1 μM Alexa Fluor 633 hydrazide, respectively, for 20 min. Arteries were excited at 405, 488, 546 and 633 nm. The emitted fluorescence was collected from cells through the bottom wall of the artery through a water immersion objective (40×) and acquired

using Olympus FluoView 1000 software (FV10-ASW). Z-stacks through the wall of the artery were obtained in 0.25 μm increments and reconstructed using Imaris, version 5.5 (Bitplane, Concord, MA, USA).

EC tube isolation

EC tubes were isolated as described previously (Socha *et al.* 2011; Socha and Segal, 2013; Garland *et al.* 2017), with modifications made for isolation from mouse mesenteric arteries. Arteries were dissected in cold dissection buffer containing (in mM): 137.0 NaCl, 5.6 KCl, 1.0 MgCl_2 , 10.0 Hepes, 10.0 glucose, 0.01 sodium nitroprusside and 0.1% BSA. Second- and third-order mesenteric arteries were dissected free of surrounding tissue. One end of the artery was cannulated onto a glass micropipette (external diameter 100–120 μm) and the lumen flushed with cold dissection buffer to remove blood. Arteries were cut into 2–3 mm segments and transferred to a clear 1.5 mL microcentrifuge tube containing 1 mL of cold dissection buffer. Artery segments were washed twice with enzyme free dissociation buffer containing (in mM): 137.0 NaCl, 5.6 KCl, 1.0 MgCl_2 , 10.0 Hepes, 10.0 glucose, 2.0 CaCl_2 and 0.1% BSA at 37°C. Segments were then incubated in dissociation buffer supplemented with 0.62 mg mL^{-1} papain, 1.0 mg mL^{-1} dithioerythritol and 1.5 mg mL^{-1} collagenase for 20–25 min at 37°C. Enzymatic digestion was terminated by aspiration of enzyme containing buffer and replaced with enzyme free dissociation buffer in a round culture dish for trituration. EC tubes were dissociated from surrounding vascular smooth muscle cells by gentle trituration using a glass micropipette (inner diameter 80–110 μm). A nanolitre injector (Nanoliter 2010) coupled with a Micro4 controller (World Precision Instruments, Sarasota, FL, USA) was mounted on an upright Olympus BX51WI microscope to allow for real-time visualization of the trituration process.

RNA extraction and quantitative RT-PCR

Arteries and EC tubes were isolated as described above. Four segments of second- and third-order artery branches from one animal were pooled for each n value. Arteries were homogenized and RNA was extracted using the RNeasy plus Mini Kit (Qiagen, Valencia, CA, USA). For EC tubes, three >1 mm long EC tubes were pooled from one animal for each n value. Isolated EC tubes were transferred using a new glass micropipette into a clean round culture dish containing enzyme free dissociation buffer, and repeated three times to reduce VSMC contamination. RNA was then extracted from EC tubes using Cells-to-CT 1-Step TaqMan Kit lysis buffer (ThermoFisher Scientific) in accordance with the manufacturer's instructions.

Quantitative RT-PCR was carried out using the Cells-to-CT 1-Step TaqMan Kit. Pre-validated, gene specific FAM-conjugated Taqman probes were purchased from ThermoFisher Scientific (Table 1). Reverse transcription was performed at 50°C for 20 min, followed by heat activation of Taq polymerase at 95°C for 30 s. PCR thermocycling conditions comprised 95°C for 15 s, then 60°C for 1 min, for 40 cycles, using the 7500 Fast Real-Time PCR system (ThermoFisher Scientific). All samples were run in duplicates along with a no template negative control for each gene. Two housekeeping genes (*Actb* and β_2M) were used to normalize gene expression. The relative expression was calculated using the ΔC_t method [$\Delta C_t = C_{t(\text{target gene})} - C_{t(\text{housekeeping gene})}$]. Success of VSMC removal was assessed by the expression of VSMC marker *Acta2* (α -SMA). $C_t > 37$ was considered not to be detected.

Drugs

All other drugs were purchased from Sigma (St Louis, MO, USA), except mouse VEGF-A₁₆₄ (#493-MV-005) (R&D Systems, Minneapolis, MN, USA); diethylamin NON-Oate (#82100; DEA NONOate), ZM323881 (#2475) and UO126 (#1144) (Tocris Bioscience, St Louis, MO, USA); Apamin (#L8407) (Latoxan, Portes-lès-Valence, France); and SLIGRL (Auspep, Tullamarine, VIC, Australia). Stock solutions of ZM323881, UO126 and TRAM-34 were prepared in DMSO and DEA NONOate in 10 mM NaOH. All other stock solutions were prepared in purified water.

Statistical analysis

All data are summarized as the mean \pm SEM of n arteries (one per animal). The Ca^{2+} events data represent the analysis of at least seven cells per artery and values were averaged to provide one n value. Only active cells were used in the calculation of frequency. Statistical comparisons were made in Prism, version 7 (GraphPad Software Inc., San Diego, CA, USA) using an unpaired Student's t test, as well as one- or two-way ANOVA with Bonferonni's *post hoc* test as appropriate. $P < 0.05$ was considered statistically significant.

Results

VEGF receptors are present in mouse resistance artery endothelial cells

RNA was extracted from either freshly isolated mesenteric arteries or from ECs alone isolated in the form of intact EC tubes. *Pecam-1* and *Acta2* were used as EC and VSMC markers, respectively. *Pecam-1* expression was evident in both intact arteries and EC tubes, whereas the *Acta2* signal

Table 1. Gene specific FAM-conjugated Taqman primers

Gene	Protein	Assay ID
<i>Pecam-1</i>	Platelet endothelial cell adhesion molecule-1 (PECAM-1)	Mm0124576.m1
<i>Acta2</i>	α -Smooth muscle actin (α -SMA)	Mm01204962.gh
β_2M	β_2 microglobulin (β_2M)	Mm00437762.m1
<i>Actb</i>	β -actin	Mm04394036.g1
<i>Flt1</i>	Vascular endothelial growth factor receptor 1 (VEGFR1)	Mm00438980.m1
<i>Flk1</i>	Vascular endothelial growth factor receptor 2 (VEGFR2)	Mm01222435.m1
<i>Nrp1</i>	Neuropilin-1 (NRP-1)	Mm00435379.m1
<i>F2r1</i>	Protease-activated receptor 2 (PAR2)	Mm00433160.m1
<i>Itpr1</i>	Inositol trisphosphate receptor 1 (IP ₃ R1)	Mm00439907.m1
<i>Itpr2</i>	Inositol trisphosphate receptor 2 (IP ₃ R2)	Mm00444937.m1
<i>Itpr3</i>	Inositol trisphosphate receptor 3 (IP ₃ R3)	Mm01306070.m1

was effectively absent from EC tubes, indicating that the EC samples were free from SMCs (Fig. 1A). *Flt1*, *Flk1* and their co-receptor *Nrp1* were each expressed in the EC tubes (Fig. 1B). Despite the presence of VEGF receptors and functional endothelium, luminal perfusion of 0.1 or 1 nM VEGF-A did not result in vasodilatation of arteries constricted with the α_1 -adrenoceptor agonist PE (Fig. 1C).

VEGF-A inhibits EDH-mediated vasodilatation to SLIGRL

We investigated whether prolonged luminal exposure to 1 nM VEGF-A, a concentration known to effectively activate VEGFR2 in rat arteries (Itoh *et al.* 2002; Egholm *et al.* 2016), might alter endothelium-dependent vasodilatation to other agonists in small resistance arteries. SLIGRL readily dilates mouse resistance arteries via the EDH-pathway and, to a lesser extent, NO (McGuire *et al.* 2002; Beleznaï *et al.* 2011). Perfusion of 1 nM VEGF-A for 60 min right-shifted the concentration response curve to SLIGRL by >2.5-fold (log EC₅₀ -5.37 ± 0.02 , $n = 12$) compared to vehicle (log EC₅₀ -5.79 ± 0.01 , $n = 8$), an effect that was not evident when arteries were perfused with 1 pM or 0.1 nM VEGF-A (Fig. 2A). The maximum dilatation to SLIGRL was not affected by 1 nM VEGF-A (E_{Max} $99.9 \pm 0.1\%$, $n = 12$; vehicle: $99.6 \pm 0.4\%$, $n = 8$).

To establish whether VEGF-A affected the NO and/or EDH pathway, the NO synthase inhibitor L-NAME was used. L-NAME had no effect on SLIGRL-mediated dilatation either when added alone or in the additional presence of VEGF-A (Fig. 2B), showing that inhibition of the NO pathway is not responsible for the inhibition of SLIGRL-mediated vasodilatation by 1 nM VEGF-A. Direct relaxation of VSMCs using the NO donor, DEA NONOate, was also unaltered by VEGF-A (Fig. 2C).

Because EC IK_{Ca} and SK_{Ca} channel activation underlies EDH-evoked vasodilatation, their role was explored using

NS309, a positive modulator of both channels. We tested the selectivity of NS309 to mediate vasodilatation via IK_{Ca} and SK_{Ca} channels using TRAM-34 and apamin (Fig. 2D). At 1 μM , NS309-mediated vasodilatation was solely dependent on IK_{Ca} and SK_{Ca} activation. Approximately 70% of the vasodilatation to 3 μM NS309 was inhibited by IK_{Ca} and SK_{Ca} blockade, whereas a significant level of vasodilatation appeared to be independent of K_{Ca} channel activity at 10 μM (Fig. 2D). Vasodilatation to NS309 was not altered by VEGF-A at 1 and 3 μM NS309 (Fig. 2D), suggesting the target may be upstream of EC K_{Ca} channels.

The effect of inhibition of IK_{Ca} and/or SK_{Ca} channels was then assessed against EDH using 1 μM TRAM-34 and 100 nM apamin, respectively. Blocking IK_{Ca} with 1 μM TRAM-34 reduced the EDH component of SLIGRL-mediated vasodilatation to a level similar to VEGF-A perfusion alone (Fig. 3A). TRAM-34 also attenuated SLIGRL-mediated vasodilatation following VEGF-A perfusion, although the effect was noticeably smaller compared to the vehicle perfused artery. The inhibitory effect against SLIGRL-mediated vasodilatation was greater with the combined treatment of VEGF-A perfusion and TRAM-34 than with VEGF-A alone. By contrast, SK_{Ca} inhibition with apamin did not affect SLIGRL-mediated dilatation in the vehicle control group but markedly inhibited vasodilatation in VEGF-A treated arteries, and more effectively than with VEGF-A and TRAM-34 (Fig. 3B). Thus, when SK_{Ca} channels were blocked and EDH-vasodilatation to SLIGRL depends on IK_{Ca} activation, VEGF-A had a pronounced inhibitory effect. When both IK_{Ca} and SK_{Ca} were inhibited, vasodilatation to SLIGRL was significantly reduced compared to inhibition of either IK_{Ca} or SK_{Ca} channels alone, consistent with vasodilatation occurring via EDH. Under these conditions, the ability of VEGF-A to inhibit SLIGRL-mediated vasodilatation was lost (Fig. 3C and D).

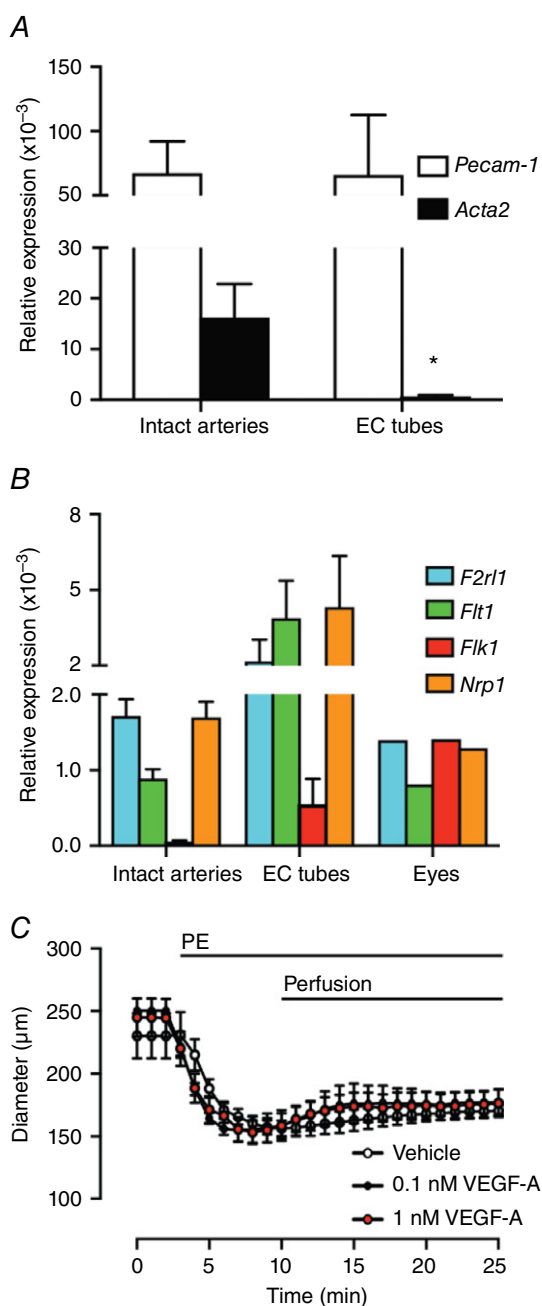


Figure 1. VEGF-A receptor expression in mouse mesenteric resistance arteries

A, *Pecam-1* and *Acta2* expression in intact arteries and isolated EC tubes. B, *Flt1*, *Flk1* and *Nrp1* expression ($n = 4$ animals). Eyes from a single animal were used as a positive control for the VEGF-A receptors. C, arteries were pre-constricted with PE. When pumped into the lumen of arteries, neither vehicle, nor VEGF-A dilated the artery within 15 min ($n = 3-4$). * $P < 0.05$ compared to intact arteries.

EC Ca²⁺ signalling was inhibited by VEGF-A exposure

Consistent with our previous studies, SLIGRL increased whole cell EC Ca²⁺ in pressurized murine mesenteric arteries associated with propagating waves (Fig. 4A). In vehicle-perfused control arteries, EC Ca²⁺ events developed locally then propagated along the cell (Ca²⁺ waves) (Fig. 4A). By contrast, luminal perfusion with 1 nM VEGF-A prevented local Ca²⁺ from evolving into propagating events (Figs 4 and 5A and D). By examining each Ca²⁺ event separately, we observed the wave events propagating at least 20 μm from where the Ca²⁺ originated in the vehicle perfused arteries, although this propagation was absent in the VEGF-A treated arteries in simulated with 3 μM SLIGRL (Fig. 5A).

Overall, VEGF-A had a marked effect on the profile of Ca²⁺ events evoked by SLIGRL, reducing the number of active cells, the frequency of Ca²⁺ events and Ca²⁺ waves (Fig. 5).

VEGFR2-MEK1/2 signalling is necessary for inhibition of both SLIGRL-mediated vasodilatation and EC Ca²⁺ activity

To identify the mechanism responsible for attenuating EDH-mediated vasodilatation, either 10 nM ZM323881, a selective VEGFR2 tyrosine kinase inhibitor (Whittles *et al.* 2002), or 10 μM UO126 (Boscolo, Mulliken and Bischoff, 2011), a selective blocker of MEK1/2, were used. The concentrations of ZM323881 and UO126 used have been demonstrated to selectively inhibit VEGFR2 and MEK1/2, respectively (Whittles *et al.* 2002; Tran and Neary, 2006; Boscolo, Mulliken and Bischoff, 2011). In each case, the inhibitory effects of VEGF-A on EC Ca²⁺ handling and vasodilatation were prevented (Fig. 6), consistent with a central role for ERK1/2 downstream of VEGFR2 in the regulation of EC Ca²⁺ and the subsequent vasodilatation in response to SLIGRL.

IP₃R1 distribution in ECs

The expression of *Itpr1-3* was found in freshly isolated intact arteries and EC tubes (Fig. 7A). IP₃R1 within ECs appeared as punctate strings forming a net-like arrangement across the cells and along the cell borders. Clusters of IP₃R1 were sometimes observed. There was no obvious change in IP₃R1 distribution following 60 min perfusion with vehicle or 1 nM VEGF-A (Fig. 7B). ZO-1 was used to distinguish the EC cell border and junctional integrity, and there was no change in ZO-1 distribution following VEGF-A perfusion.

Discussion

The present study provides evidence that prolonged stimulation with VEGF-A, through the activation of VEGFR2 and the MEK1/2 pathway, inhibits EC Ca^{2+} mobilization and agonist-evoked vasodilatation in mouse mesenteric resistance arteries. The altered Ca^{2+} handling prevented the effective activation of EC K_{Ca} channels, in particular IK_{Ca} , reducing the subsequent EDH-mediated vasodilatation.

The majority of studies on the arterial action of VEGF-A have focussed primarily on its acute role as a vasodilator. Longer-term effects of VEGF-A have not been reported, despite the fact that VEGF-A is elevated chronically in numerous pathological conditions, including peripheral artery disease, diabetes associated complications and pre-eclampsia (Baker *et al.* 1995; Stehr *et al.* 2010). Furthermore, high serum VEGF-A has been linked to an increased likelihood of detrimental cardiovascular events (Kaess *et al.* 2016). Most studies rely on an antibody based enzyme linked immunosorbent assay to detect VEGF-A in the blood. However, both the type of sample (serum/plasma) and the circulating levels of

soluble VEGFR1 and VEGFR2 affect VEGF-A binding to antibodies and, as such, reduce our ability to accurately determine the concentration of circulating VEGF-A. Thus, the reported normal level for VEGF-A in the blood ranges from undetectable to ~ 100 pM, with values that can increase into the nanomolar range in cancer and pre-eclampsia patients (Baker *et al.* 1995; Takahashi *et al.* 1995; Larsson, Sköldenberg and Eericson, 2002). In the present study, we used 1 nM VEGF-A, which is known to effectively activate VEGFR2 and cause vasodilatation in a number of different vascular beds (Itoh *et al.* 2002; Egholm *et al.* 2016).

Using a previously established method to isolate fresh ECs rapidly from mesenteric arteries (Socha *et al.* 2011), we detected both VEGFR and NRP-1 expression, confirming the presence of VEGF receptors in the ECs of resistance arteries. However, despite the presence of a functional endothelium and VEGFRs, we were unable to evoke vasodilatation with VEGF-A in mouse mesenteric arteries. The VEGF-A level rises gradually with perfusion, with the concentration peaking ~ 5 min following the arrival of VEGF-A in the lumen. Vasodilatation was not

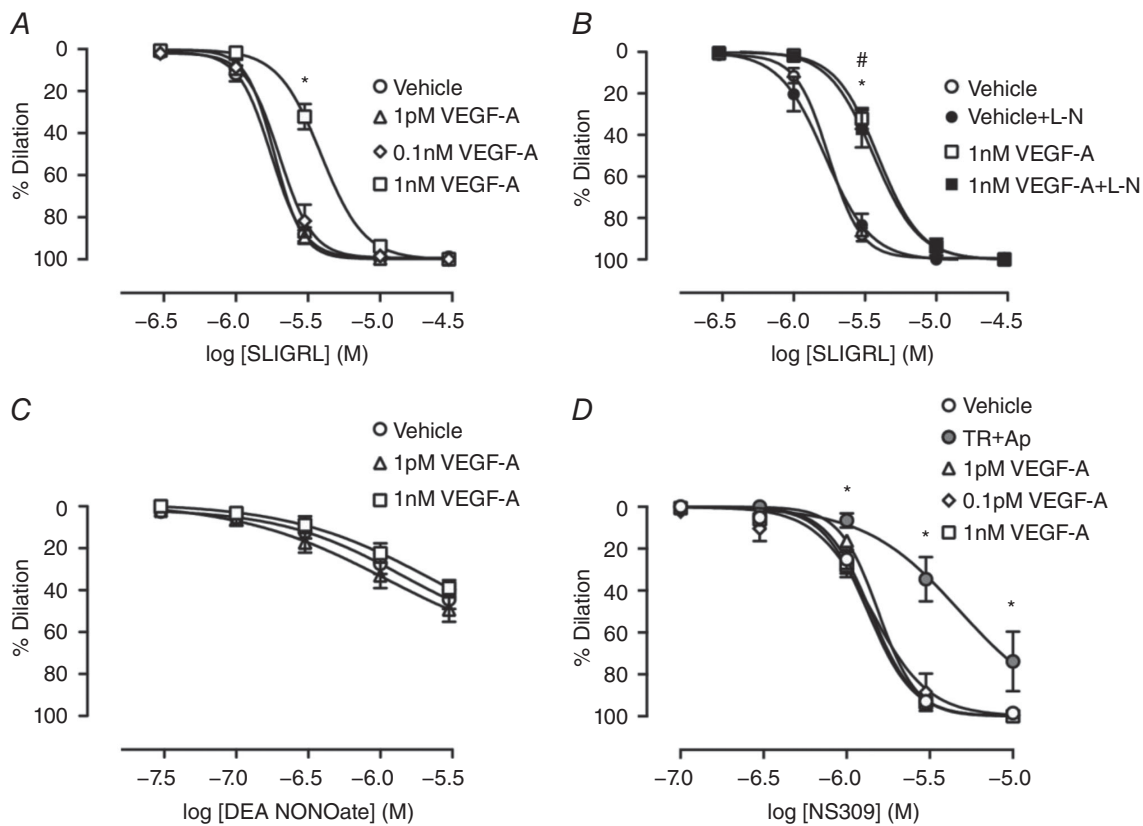


Figure 2. VEGF-A inhibits EDH-mediated vasodilatation evoked by SLIGRL
 Arteries were perfused with either vehicle or VEGF-A for 60 min. A, vasodilatation to SLIGRL ($n = 7-8$). B, vasodilatation to SLIGRL in the presence of L-NAME (L-N) ($n = 5-8$). C, vasodilatation to DEA NONOate ($n = 7-9$). D, vasodilatation to NS309 ($n = 3-12$). TR, TRAM-34; Ap, apamin. * $P < 0.05$ compared to vehicle. # $P < 0.05$ compared to vehicle + L-N.

observed at any point, suggesting that neither low, nor high concentrations of VEGF-A led to vasodilatation in mouse mesenteric arteries. In other vascular beds, VEGF-A evoked vasodilatation is slow, often requiring 10–15 min before an effect is observed, which appears to be NO-dependent. Because we found that exogenous NO only evoked moderate vasodilatation of mouse mesenteric arteries, the lack of vasodilatation to VEGF-A may simply reflect a lack of responsiveness in this artery. Although it has been reported that VEGF-A can cause vasoconstriction once NOS is blocked (Egholm *et al.* 2016), we did not observe this phenomenon.

Despite a low arterial sensitivity to NO, SLIGRL evokes pronounced EC-dependent vasodilatation via EDH (McGuire *et al.* 2002). This vasodilatation was inhibited after 60 min of exposure to VEGF-A, showing the growth factor can negatively and significantly attenuate EDH-vasodilatation. The inhibitory action of VEGF-A did not increase further during repeated dose response curves ~1 h later and in the presence of L-NAME. This ability of VEGF-A to reduce vasodilatation does not appear to be restricted to SLIGRL, and other studies have observed reduced vasodilatation to bradykinin using human dermal resistance arteries (Svedas *et al.* 2003).

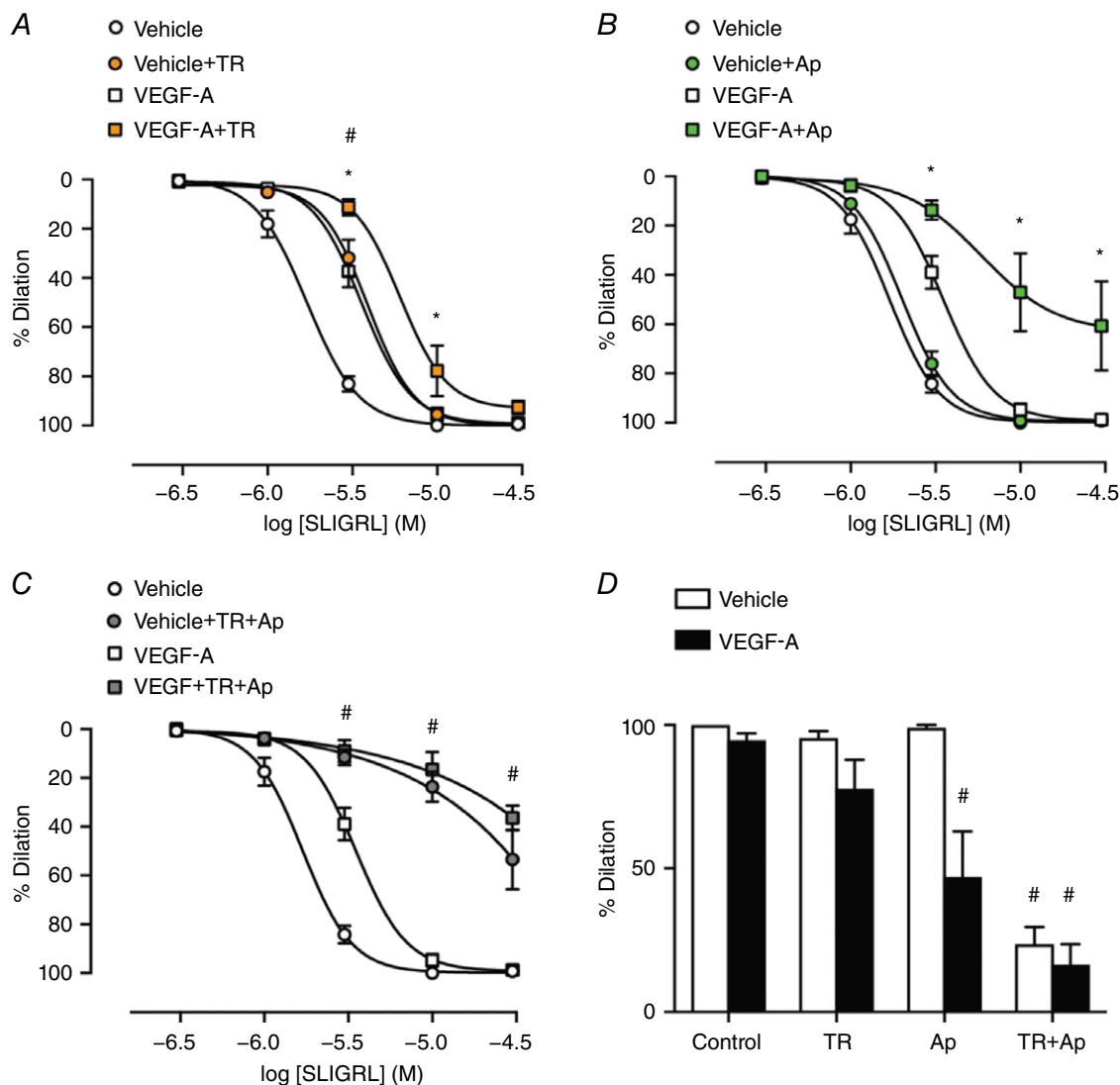


Figure 3. VEGF-A inhibits IKCa and SKCa-dependent EDH vasodilatation

Arteries were perfused with either vehicle or 1 nM VEGF-A for 60 min. All experiments were performed in the presence of L-NAME. Vehicle and VEGF-A are from Fig. 2. *A*, vasodilatation to SLIGRL with the addition of TRAM-34 (TR) ($n = 5-13$). *B*, vasodilatation with the addition of apamin (Ap) ($n = 3-13$). *C*, SLIGRL-mediated vasodilatation in the presence of TRAM-34 and apamin ($n = 3-13$). *D*, vasodilatation to 10 μM SLIGRL in the presence of IKCa and SKCa inhibitors. * $P < 0.05$ compared to VEGF-A. # $P < 0.05$ compared to vehicle + TR.

Supporting an inhibitory action against vasodilatation as a general mechanism and that high-dose VEGF-A infusion can cause a sustained increase in systemic vascular resistance (Yang *et al.* 1998).

SLIGRL-evoked vasodilatation in mesenteric arteries from wild-type mice relies on EDH, which is mediated

by K^+ efflux through EC IK_{Ca} and SK_{Ca} channels (Dora *et al.* 2003; Beleznai *et al.* 2011). However, VEGF-A did not alter vasodilatation to the K_{Ca} channel opener NS309, a positive modulator of the channels, which mimics EDH-vasodilatation. Because NS309 activates both SK_{Ca} and IK_{Ca} channels, this raised the possibility VEGF-A

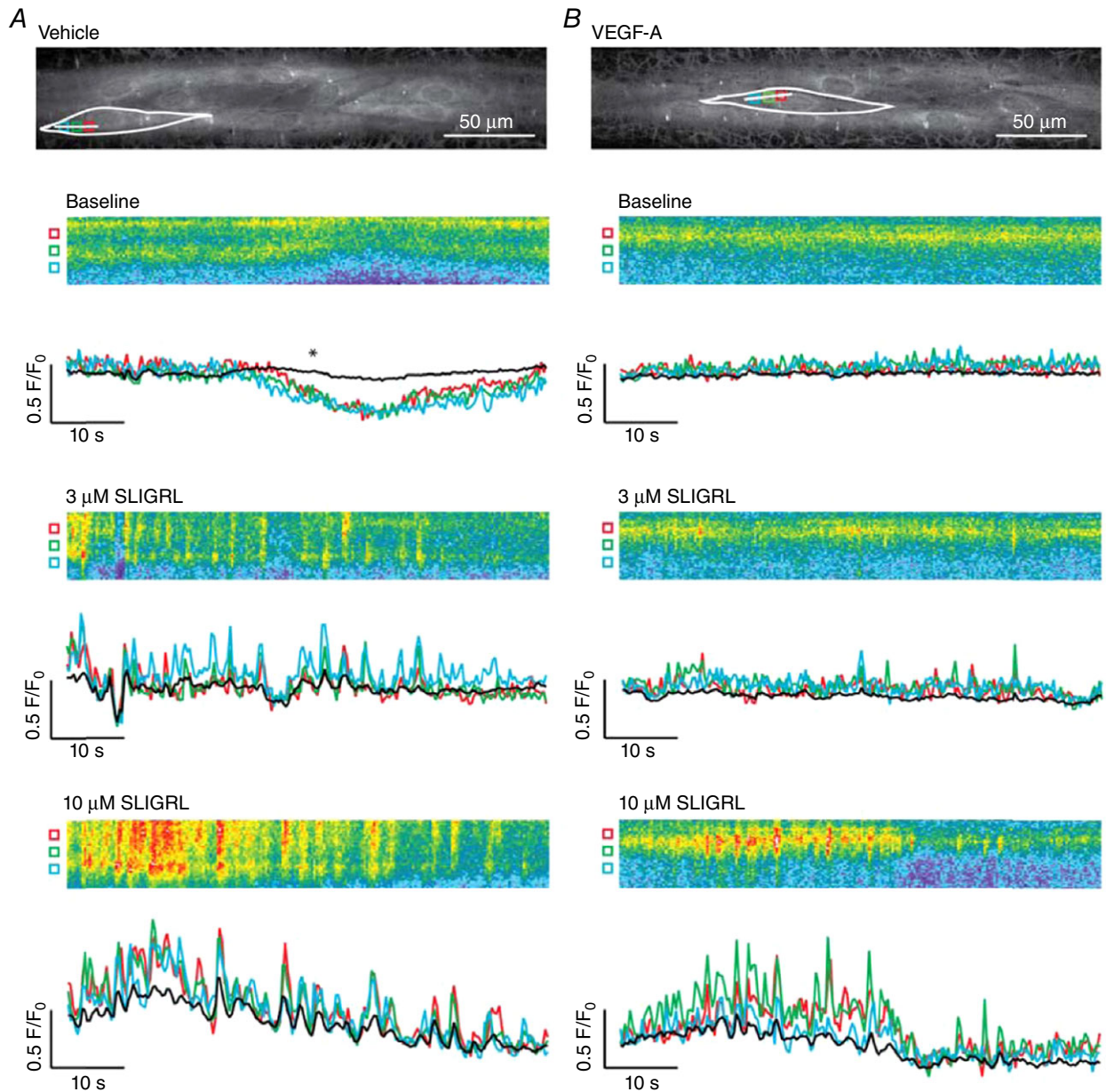


Figure 4. VEGF-A pre-exposure inhibits propagation of EC Ca^{2+}
 Pressurized arteries were lumenally perfused with vehicle or 1 nM VEGF-A for 60 min. Baseline Ca^{2+} was recorded for 1 min, SLIGRL was then added and remained in the bath for the duration of the recording. *A*, following perfusion of vehicle, 3 and 10 μ M SLIGRL stimulated a clear increase in Ca^{2+} waves along the length of the cell. *B*, following perfusion of VEGF-A, 3 μ M SLIGRL stimulated less frequent, localized Ca^{2+} events, whereas 10 μ M SLIGRL increased Ca^{2+} event frequency and Ca^{2+} waves propagated along the cell. Data are shown as line scans (corresponding to white lines in *A* and *B*) with fluorescence traces referring to subcellular regions of interest (coloured boxes in *A* and *B*). Black trace refers to whole-cell recording. *Dip in intensity as a result of a movement artefact. Representative of five or six independent experiments.

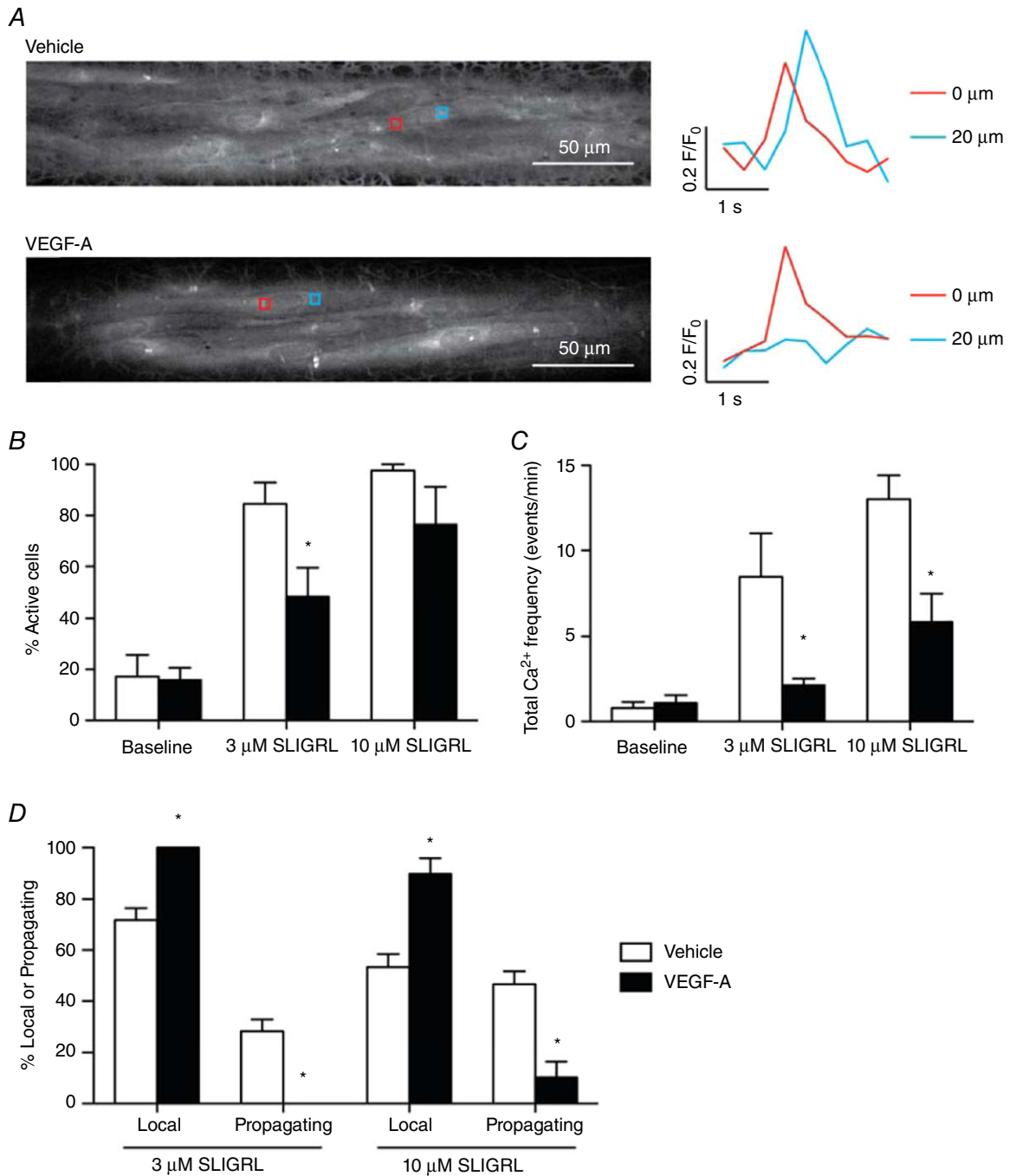


Figure 5. VEGF-A inhibits SLIGRL-mediated Ca^{2+} events and wave propagation

A, arteries were stimulated with 3 μM SLIGRL. Regions of interests were positioned 20 μm apart in active ECs: upper: vehicle perfused with trace to right showing a propagating wave; lower: 1 nM VEGF-A perfused with a local event shown to the right. Representative of multiple cells within five or six independent experiments. B–D, summary of Ca^{2+} events. Following luminal perfusion with 1 nM VEGF-A for 60 min, fewer ECs respond to 3 μM SLIGRL (B) and, of the active cells, there were fewer Ca^{2+} events (C). D, VEGF-A treated arteries produced fewer propagating Ca^{2+} events compared to the vehicle-treated arteries. $n = 5–6$; * $P < 0.05$ compared to vehicle.

modifies the input of only one type of channel. EC SK_{Ca} inhibition with apamin had a profound effect on SLIGRL-mediated vasodilatation, although only following exposure to VEGF-A, suggesting the growth factor targets IK_{Ca} to reduce vasodilatation. Interestingly, TRAM-34 right-shifted the SLIGRL (control) vasodilatation curve, indicating a predominant role for these channels in EDH-vasodilatation, and contrasting with the absence of a similar shift when SK_{Ca} channels were blocked with apamin. Following VEGF-A perfusion, there remained a small EDH component sensitive to TRAM-34 inhibition. This suggests that VEGF-A did not completely abolish the IK_{Ca} response. EDH-vasodilatation was abolished by combined blockade of IK_{Ca} and SK_{Ca} and, not surprisingly, there was no inhibitory effect with VEGF-A, highlighting EDH as the target for VEGF-A mediated attenuation.

Boeldt *et al.* (2017) previously reported that VEGF-A can affect connexin 43, which can inhibit the spread of hyperpolarizing current to mediate vasodilatation. However, the fact that NS309-mediated vasodilatation was not modified at all by VEGF-A suggests that current propagation and the EC K_{Ca} channels may not be the

primary target for VEGF-A attenuation. This raised the possibility that the inhibitory target was downstream of PAR2 receptor activation but upstream of K_{Ca} channels. SLIGRL acts through PAR2 to induce Ca²⁺ release via IP₃Rs, with these Ca²⁺ events evolving into propagating waves spreading across the ECs. However, following exposure to VEGF-A, the number of cells responding to SLIGRL was reduced and the underlying Ca²⁺ events became localized to smaller, more restricted sites. The restriction of Ca²⁺ release after exposure to VEGF-A translated to a reduced global increase of Ca²⁺, which would be predicted to compromise the effective opening of EC K_{Ca} channels and thus reduce EDH-vasodilatation. Although both IK_{Ca} and the SK_{Ca} channels are probably affected by the reduction in Ca²⁺ release, the reduction appeared to be particularly pronounced with IK_{Ca} input to EDH because, once SK_{Ca} channels were inhibited by apamin, the ability of SLIGRL to fully dilate arteries was dramatically reduced by prolonged exposure to VEGF-A. The greater impact of IK_{Ca} blockade may reflect that these channels are localized in the fine myoendothelial projections, where ECs make contact with the VSMCs, whereas the SK_{Ca} channels are more uniformly distributed across the membrane (Dora

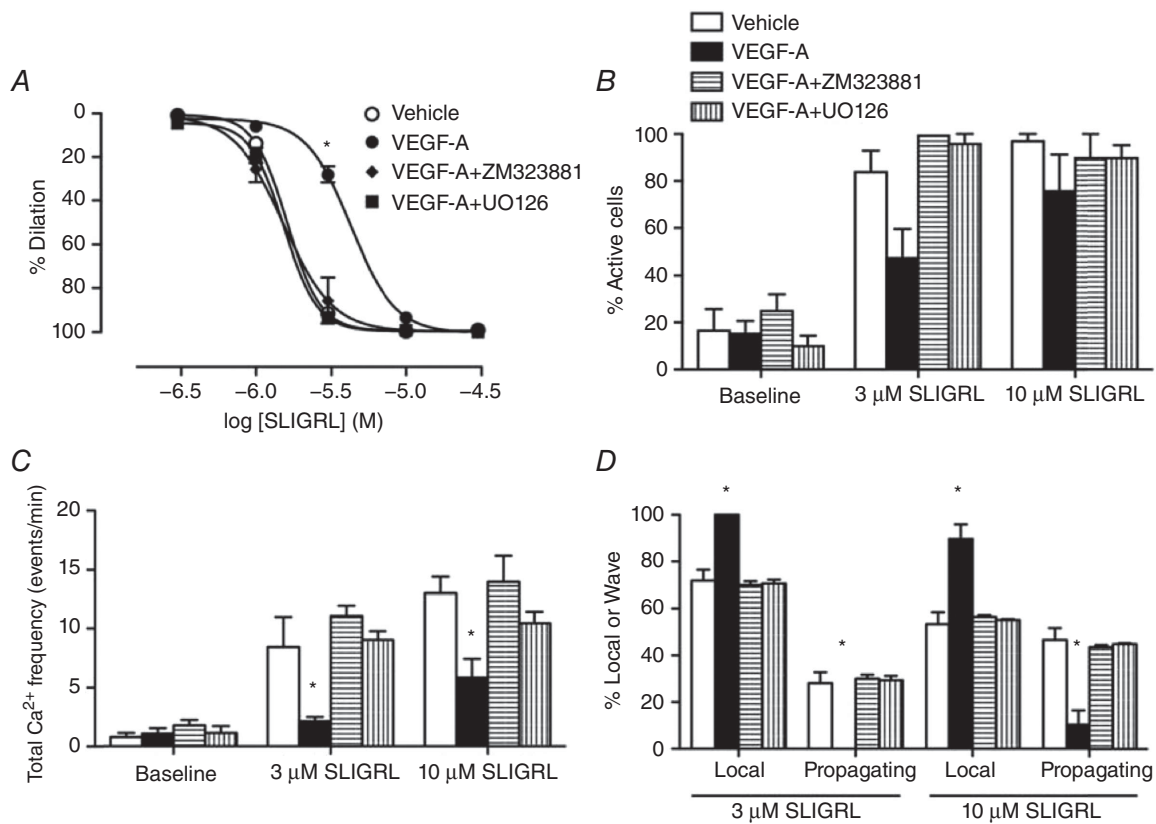


Figure 6. VEGF-A inhibits SLIGRL-mediated EC Ca²⁺ events and vasodilatation via ERK1/2 signalling
 Vehicle and VEGF-A are from Fig. 5. Arteries were perfused with either vehicle or 1 nM VEGF-A with and without inhibitors for 60 min. A, ZM323881 and UO126 prevented VEGF-A induced inhibition of SLIGRL-mediated vasodilatation (n = 3–12). B–D, quantification of EC Ca²⁺ activities in arteries treated with ZM323881 or UO126 (n = 3–6). *P < 0.05 compared to vehicle.

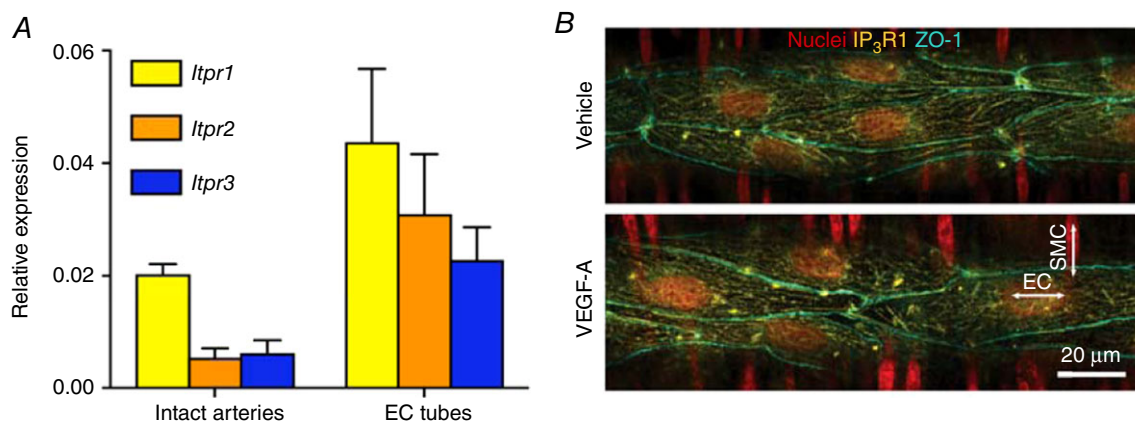


Figure 7. Distribution of IP₃R1 in ECs is not modified by VEGF-A

A, *Itpr1-3* expression in intact arteries and EC tubes ($n = 4$). *B*, pressurized arteries were perfused with either vehicle or 1 nM VEGF-A for 60 min. Immunolabelling showed the IP₃R1 distribution in ECs (horizontal nuclei). The distribution of ZO-1 appears to be unaltered by VEGF-A in arteries. Representative of three arteries per treatment.

et al. 2008). In HUVECs, other studies have reported that 250 pM VEGF-A reduced the ATP-mediated increase in frequency of Ca²⁺ bursts and [Ca²⁺]_i (Boeldt *et al.* 2017). Therefore, it appears the effects of VEGF-A are not limited to PAR2-receptor mediated responses.

MEK1/2 signalling (and subsequent activation of ERK1/2) is a major signalling pathway downstream of VEGFR2 activation and it appears to be essential for VEGF-A to exert an inhibitory effect on EC Ca²⁺ release. This suggests that ERK1/2, a serine/threonine kinase, may have a direct role in the regulation of EC Ca²⁺. Other studies suggest that ERK phosphorylates S⁴³⁶ of IP₃R1 to reduce Ca²⁺ release and the frequency of Ca²⁺ oscillations (Bai *et al.* 2006). This ERK1/2 phosphorylation site is absent in both IP₃R2 and IP₃R3 (Bai *et al.* 2006; Yang *et al.* 2006), which supports the possibility that SLIGRL-mediated Ca²⁺ release and propagation are largely dependent on IP₃R1 in the present study. When we examined the localization and distribution of IP₃R1, we did not observe any obvious changes, and so altered Ca²⁺ signalling was probably not caused by a redistribution of IP₃R1. However, once appropriate phospho-specific antibodies to IP₃R1 become available for immunolabelling, it will be interesting to establish whether the IP₃R1 is phosphorylated during exposure to VEGF-A in pressurized artery ECs, as well as on which residues this occurs.

Our understanding of VEGF-A signalling in the resistance vasculature is far from complete. The majority of data available have focussed on capillaries and the ability of VEGF-A to evoke arterial vasodilatation. As a result of its angiogenic and pro-survival properties in ECs, VEGF-A has been trialled as a mean to stimulate therapeutic re-vascularization. Although early studies that suggest VEGF-A improves myocardial outcome in patients, the

benefits of this approach were far less clear in later, more stringent trials (Losordo *et al.* 2002; Stewart *et al.* 2009). Although it has been suggested that VEGF-A may reduce NO release evoked by other EC-dependent vasodilators *in vitro* (Boeldt *et al.* 2017), the present study provides the first functional evidence to suggest that long-term exposure to VEGF-A prevents effective vasodilatation and that it does this by disrupting EDH-vasodilatation. As such, VEGF-A has the potential to increase peripheral resistance and compromise tissue blood flow, which may counteract any potential benefit of therapeutic angiogenesis.

References

- Bagher, P., Davis, M. and Segal, S. (2011). Visualizing calcium responses to acetylcholine convection along endothelium of arterolar networks in Cx40^{BAC}-GCaMP2 transgenic mice. *Am J Physiol Heart Circ Physiol* **301**, H794–H802.
- Bai, G.-R., Yang, L.-H., Huang, X.-Y. and Sun, F.-Z. (2006). Inositol 1,4,5-trisphosphate receptor type 1 phosphorylation and regulation by extracellular signal-regulated kinase. *Biochem Biophys Res Commun* **348**, 1319–1327.
- Baker, P., Krasnow, J., Roberts, J. and Yeo, K. (1995). Elevated serum levels of vascular endothelial growth factor in patients with preeclampsia. *Obstet Gynecol* **86**, 815–21.
- Beleznai, T., Takano, H., Hamill, C., Yarova, P., Douglas, G., Channon, K. and Dora, K. (2011). Enhanced K⁺-channel-mediated endothelium-dependent local and conducted dilation of small mesenteric arteries from ApoE^{-/-} mice. *Cardiovasc Res* **92**, 199–208.
- Boeldt, D. S., Krupp, J., Yi, F. X., Khurshid, N., Shah, D. M. and Bird, I. M. (2017). Positive versus negative effects of VEGF₁₆₅ on Ca²⁺ signaling and NO production in human endothelial cells. *Am J Physiol Heart Circ Physiol* **312**, H173–H181.

- Boscolo, E., Mulliken, J. B. and Bischoff, J. (2011). VEGFR-1 mediates endothelial differentiation and formation of blood vessels in a murine model of infantile hemangioma. *Am J Pathol* **179**, 2266–77.
- Cheng, H., James, A., Foster, R., Hancox, J. and Bates, D. (2006). VEGF activates receptor-operated cation channels in human microvascular endothelial cells. *Arterioscler Thromb Vasc Biol* **26**, 1768–76.
- Dora, K. A., Gallagher, N. T., Mcneish, A. and Garland, C. J. (2008). Modulation of endothelial cell KCa3.1 channels during endothelium-derived hyperpolarizing factor signaling in mesenteric resistance arteries. *Circ Res* **102**, 1247–1255.
- Dora, K., Sandow, S., Gallagher, N., Takano, H., Rummery, N., Hill, C. and Garland, C. (2003). Myoendothelial gap junctions may provide the pathway for EDHF in mouse mesenteric artery. *J Vasc Res* **40**, 480–90.
- Edwards, G., Dora, K., Gardener, M., Garland, C. and Weston, A. (1998). K⁺ is an endothelium-derived hyperpolarizing factor in rat arteries. *Nature* **396**, 269–272.
- Egholm, C., Khammy, M. M., Dalsgaard, T., Mazur, A., Tritsarlis, K., Hansen, A. J., Aalkjaer, C. and Dissing, X. S. (2016). GLP-1 inhibits VEGFA-mediated signaling in isolated human endothelial cells and VEGFA-induced dilation of rat mesenteric arteries. *Am J Physiol Heart Circ Physiol* **1311**, H1214–H1224.
- Favia, A., Desideri, M., Gambarà, G., D'Alessio, A., Ruas, M., Esposito, B., Del Bufalo, D., Parrington, J., Ziparo, E., Palombi, F., Galione, A. and Flippini, A. (2014). VEGF-induced neoangiogenesis is mediated by NAADP. *Proc Natl Acad Sci U S A* **111**, E4706–15.
- Fong, G., Rossant, J., Gertsenstein, M. and Breitman, M. (1995). Role of the Flt-1 receptor tyrosine kinase in regulating the assembly of vascular endothelium. *Nature* **376**, 66–70.
- Garland, C. J., Bagher, P., Powell, C., Ye, X., Lemmey, H. A. L., Borysova, L. and Dora, K. A. (2017). Voltage-dependent Ca²⁺ entry into smooth muscle during contraction promotes endothelium-mediated feedback vasodilation in arterioles. *Sci Signal* **10**, eaal3806.
- Garland, C. J. and Dora, K. A. (2017). EDH: endothelium-dependent hyperpolarization and microvascular signalling. *Acta Physiol (Oxf)* **219**, 152–161.
- Goel, H. L. and Mercurio, A. M. (2013). VEGF targets the tumour cell. *Nat Rev Cancer* **13**, 871–82.
- Grundy, D. (2015). Principles and standards for reporting animal experiments in The Journal of Physiology and Experimental Physiology. *J Physiol* **593**, 2547–2549.
- Hamdollah Zadeh, M., Glass, C. A., Magnussen, A., Hancox, J. and Bates, D. O. (2008). VEGF-mediated elevated intracellular calcium and angiogenesis in human microvascular endothelial cells in vitro are inhibited by dominant negative TRPC6. *Microcirculation* **15**, 605–614.
- Itoh, S., Brawley, L., Wheeler, T., Anthony, F. W., Poston, L. and Hanson, M. A. (2002). Vasodilation to vascular endothelial growth factor in the uterine artery of the pregnant rat is blunted by low dietary protein intake. *Pediatr Res* **51**, 485–491.
- Jang, K., Kim, M., Gilbert, C. A., Simpkins, F., Ince, T. A. and Slingerland, J. M. (2017). VEGFA activates an epigenetic pathway upregulating ovarian cancer-initiating cells. *EMBO Mol Med* **9**, 304–318.
- Kaess, B. M., Preis, S. R., Beiser, A., Sawyer, D. B., Chen, T. C., Seshadri, S. and Vasan, R. S. (2016). Circulating vascular endothelial growth factor and the risk of cardiovascular events. *Heart* **102**, 1898–1901.
- Kawamura, H., Li, X., Harper, S. J., Bates, D. O. and Claesson-Welsh, L. (2008). Vascular endothelial growth factor (VEGF)-A_{165b} is a weak in vitro agonist for VEGF receptor-2 due to lack of coreceptor binding and deficient regulation of kinase activity. *Cancer Res* **68**, 4683–4692.
- Ku, D. D., Zaleski, J. K., Liu, S. and Brock, T. A. (1993). Vascular endothelial growth factor induces EDRF-dependent relaxation in coronary arteries. *Am J Physiol Heart Circ Physiol* **265**, H586–H592.
- Larsson, A., Sköldenberg, E. and Ericson, H. (2002). Serum and plasma levels of FGF-2 and VEGF in healthy blood donors. *Angiogenesis* **5**, 107–110.
- Lim, H., Blann, A., Chong, A., Freestone, B. and Lip, G. (2004). Plasma vascular endothelial growth factor, angiopoietin-1, and angiopoietin-2 in diabetes: implications for cardiovascular risk and effects of multifactorial intervention. *Diabetes Care* **27**, 2918–2924.
- Losordo, D. W., Vale, P. R., Hendel, R. C., Milliken, C. E., Fortuin, F. D., Cummings, N., Schatz, R. A., Asahara, T., Isner, J. M. and Kuntz, R. E. (2002). Clinical investigation and reports trial of myocardial vascular endothelial growth factor 2 gene transfer by catheter delivery in patients with chronic myocardial ischemia. *Circulation* **105**, 2012–2018.
- McGuire, J. J., Hollenberg, M. D., Andrade-Gordon, P. and Triggie, C. R. (2002). Multiple mechanisms of vascular smooth muscle relaxation by the activation of proteinase-activated receptor 2 in mouse mesenteric arterioles. *Br J Pharmacol* **135**, 155–69.
- Simons, M., Gordon, E. and Claesson-welsh, L. (2016). Mechanisms and regulation of endothelial VEGF receptor signalling. *Nat Rev Mol Cell Biol* **17**, 611–625.
- Socha, M., Hakim, C., Jackson, W. and Segal, S. (2011). Temperature effects on morphological integrity and Ca²⁺ signaling in freshly isolated murine feed artery endothelial cell tubes. *Am J Physiol Heart Circ Physiol* **301**, H773–H783.
- Socha, M. J. and Segal, S. S. (2013). Isolation of microvascular endothelial tubes from mouse resistance arteries. *J Vis Exp* **25**, e50759.
- Soker, S., Takashima, S., Miao, H. Q., Neufeld, G. and Klagsbrun, M. (1998). Neuropilin-1 is expressed by endothelial and tumor cells as an isoform-specific receptor for vascular endothelial growth factor. *Cell* **92**, 735–745.
- Stehr, A., Töpel, I., Müller, S., Unverdorben, K., Geissler, E. K., Kasprzak, P. M., Schlitt, H. J. and Steinbauer, M. (2010). VEGF: a surrogate marker for peripheral vascular disease. *Eur J Endovasc Surg* **39**, 330–332.

- Stewart, D. J., Kutryk, M. J. B., Fitchett, D., Freeman, M., Camack, N., Su, Y., Della Siega, A., Bilodeau, L., Burton, J. R. and Proulx, G. (2009). VEGF gene therapy fails to improve perfusion of ischemic myocardium in patients with advanced coronary disease: results of the NORTHERN trial. *Mol Ther* **17**, 1109–1115.
- Svedas, E., Islam, K. B., Nisell, H. and Kublickiene, K. R. (2003). Vascular endothelial growth factor induced functional and morphologic signs of endothelial dysfunction in isolated arteries from normal pregnant women. *Am J Obstet Gynecol* **188**, 168–176.
- Takahashi, Y., Kitadai, Y., Bucana, C. D., Cleary, K. R. and Ellis, L. M. (1995). Expression of vascular endothelial growth factor and its receptor, KDR, correlates with vascularity, metastasis, and proliferation of human colon cancer. *Cancer Res* **55**, 3964–3968.
- Tran, M. D. and Neary, J. T. (2006). Purinergic signaling induces thrombospondin-1 expression in astrocytes. *Proc Natl Acad Sci U S A* **103**, 9321–9326.
- Whittles, C. E., Pocock, T. M., Wedge, S. R., Kendrew, J., Hennequin, L. F., Harper, S. J. and Bates, D. O. (2002). ZM323881, a novel inhibitor of vascular endothelial growth factor-receptor-2 tyrosine kinase activity. *Microcirculation* **9**, 513–522.
- Yang, L., Bai, G., Huang, X. and Sun, F. (2006). ERK binds, phosphorylates InsP3 type 1 receptor and regulates intracellular calcium dynamics in DT40 cells. *Biochem Biophys Res Commun* **349**, 1339–1344.
- Yang, R., Bunting, S., Ko, A., Leyt, B., Modi, N., Zioncheck, T., Ferrara, N. and Jin, H. (1998). Substantially attenuated hemodynamic responses to *Escherichia coli*-derived vascular endothelial growth factor given by intravenous infusion compared with bolus injection. *J Pharmacol Exp Ther* **284**, 103–110.

Additional information

Competing interests

The authors declare that they have no competing interests.

Author contributions

XY conceived and designed the work and drafted the manuscript. XY and TB acquired, analysed and interpreted the data. PB, CJG and KAD helped design and interpret experiments and edited the manuscript. All authors approved the final version of the manuscript submitted for publication and are accountable for all aspects of the work. All persons designated as authors qualify for authorship and all those who qualify are listed.

Funding

This work was supported by the British Heart Foundation (PG/14/58/30998; FS/13/16/30199) and the Oxford BHF Centre of Research Excellence (RE/13/1/30181). KAD is a BHF-funded Senior Basic Science Research Fellow.